Localized breathing oscillations of Bose-Einstein condensates in periodic traps

R. Carretero-González[1,*] and K. Promislow[2]

[1]*Nonlinear Dynamical Systems Group,*[†] *Department of Mathematics & Statistics, San Diego State University, San Diego, California 92182-7720*

[2]*Department of Mathematics & Statistics, Simon Fraser University, Burnaby, BC, Canada V5A 1S6*

(Received 30 May 2001; published 20 September 2002)

We demonstrate the existence of localized oscillatory breathers for quasi-one-dimensional Bose-Einstein condensates confined in periodic potentials. The breathing behavior corresponds to position oscillations of individual condensates about the minima of the potential lattice. We deduce the structural stability of the localized oscillations from the construction. The stability is confirmed numerically for perturbations to the initial state of the condensate, to the potential trap, as well as for external noise. We also construct periodic and chaotic extended oscillations for the chain of condensates. All our findings are verified by direct numerical integration of the Gross-Pitaevskii equation in one dimension.

DOI: 10.1103/PhysRevA.66.033610 PACS number(s): 03.75.Fi, 05.45.−a, 52.35.Mw, 63.20.Pw

New techniques for generating Bose-Einstein condensates (BECs) have opened the door to the investigation of a wide range of phenomena and development of concrete applications such as atomic interferometers and atom lasers. Recent focus has been on BECs trapped in periodic magnetic/optical traps [1–3], the so-called optical lattice [4]. The addition of a periodic potential to the BEC opens the possibility to study exciting dynamical phenomena of BECs grown in optical traps, such as Bloch oscillations and the Josephson effect [1–3]. One approach for the study of chains of weakly coupled condensates, in the tight-binding approximation, reduces the dynamics of the BECs to the discrete nonlinear Schrödinger equation (DNLS) [2,3,5–7]. Within this approach, each BEC wave function, centered at the minima of the potential, is modeled by the *same stationary* wave function with a time-dependent amplitude. This approximation leads to the DNLS for the local time-dependent amplitudes. The dynamics described by this approach allows for variations in the local population of atoms, but are limited to a fixed local distribution of the condensed atoms. In this paper we use a more general approach where the local wave function evolves within an ansatz family, allowing for a wider range of dynamical behavior. Using the treatment presented here it is possible to include variations in the local populations as well as in the *shape* of the local density: height, width, position, phase, velocity, etc. In particular, we focus our attention on position oscillations of each *local* BEC density about its potential minimum by considering a constant population at each trough of the periodic potential. We model the coupled chain of oscillating condensates by a nonlinear lattice (a Toda lattice with on-site effective potentials) for the oscillation amplitudes. We establish the existence of global and localized oscillations of the coupled condensates, and demonstrate the ability of condensates to store macroscopic information in localized regions of the periodic trap.

*Email address: carreter@math.sdsu.edu;
URL: http://www.rohan.sdsu.edu/~rcarrete

†URL: http://nlds.sdsu.edu/

The wave function of a dilute BEC at low temperature is governed by the Gross-Pitaevskii equation (GPE) [8]

$$i\hbar\frac{\partial\psi}{\partial t}=\left(-\frac{\hbar^2\nabla^2}{2m}+V_{\rm ext}(\vec{r})+g_0|\psi|^2\right)\psi, \tag{1}$$

where $\psi=\psi(\vec{r},t)$ is the condensate wave function normalized with respect to the total number of condensed atoms $\mathcal{N}$. The atom-atom interactions (considered only binary due to the low-temperature assumption) are accounted for by the coupling constant [9]

$$g_0=\frac{4\pi\hbar^2 a}{m},$$

where a is the s-wave scattering length and m is the atomic mass. The external potential $V_{\rm ext}(\vec{r})$ is given by the sum of the confining potential $V_{\rm conf}(\vec{r})$ and a periodic optical potential $V_{\rm per}(\vec{r})$:

$$V_{\rm ext}(\vec{r})=V_{\rm conf}(\vec{r})+V_{\rm per}(\vec{r}).$$

We consider confining traps that give rise to the so-called cigar-shaped condensates whose longitudinal direction is much larger than their transverse dimension, which is of the order of the healing length. In this cigar-shaped limit it is possible to reduce the GPE equation (1) to its one-dimensional analogue [10]. Our study will be limited to the one-dimensional model of attractive BECs. Extension of our results to the repulsive BEC in one and higher dimensions will be reported elsewhere. Our model applies to the dynamics of a chain of quasi-identical condensates, in an infinite confining trap. In practice, the harmonic external trap has a flat central portion supporting several hundreds of periods of the periodic potential, which is sufficient to satisfy the desired near-periodic potential (see Fig. 1). It is also possible to load the condensate onto $V_{\rm ext}$ and then adiabatically remove $V_{\rm conf}$, leaving only the periodic potential.

After rescaling, the BEC trapped inside a periodic potential V is governed by the nonlinear Schrödinger equation (NLS):

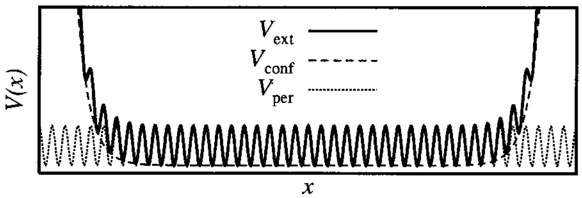

FIG. 1. External potential V_{ext} with confining (V_{conf}) and periodic $[V_{per}(x)]$ properties.

$$iu_t+\frac{1}{2}u_{xx}\pm|u|^2u=V(x)u. \tag{2}$$

Here $|u(x,t)|^2$ corresponds to the rescaled density of the condensate, $V(x)$ is the rescaled potential, and the $\pm$ sign corresponds to attractive $(+)$ and repulsive $(-)$ atoms. The nondimensionalization is obtained by scaling $t\to t/\Omega$, $x\to(\hbar/m\Omega)^{1/2}x$, and $|u|^2\to(m\Omega/4\pi\hbar|a|)|u|^2$, where m is the atomic mass, Ω is the frequency of the periodic trap, and a is the s-wave scattering length [11]. We consider a periodic potential $V(x)$, with well spaced troughs, constructed by "concatenating" $2N+1$ $(N\gg 1)$ single-well potentials $V_j(x)=V_0\tanh^2(x-\xi_{0;j})$:

$$V(x)=\sum_{j=-N}^{N}V_j(x)-2NV_0.$$

The potentials are located at $\xi_{0;j}=jR$, where R is the potential-well spacing. The specific shape of the potentials V_j is not central to the construction. However, our approximations require that neighboring condensates, grown in adjacent wells, have small overlap. This regime corresponds to large enough R or to a small number of atoms per potential well. The large R limit can be achieved by tuning the wave number of the optical trap. Alternatively, new advances in the manipulation of condensates permit the construction of traps with arbitrary spatial patterns by imprinting the pattern in a crystal by a grating method or by lithography [12].

The present paper addresses the dynamics of a chain of coupled attractive condensates, i.e., *bright* solitons. For repulsive atoms—*dark* solitons [13]—a similar approach is possible and the detailed analysis will be carried elsewhere. Current typical lifetimes for attractive condensates range from hundreds to tenths of a second before collapse. These lifetimes correspond, for typical experimental parameters in ^{85}Rb [14], to 10^3 rescaled time units, long enough to observe 10–20 oscillation periods. Moreover, new microtrap techniques [12] and hollow laser traps [15] hold out the possibility to increase considerably the lifetime of attractive condensates [16], permitting time to prepare the train of condensates with the desired phase configuration. It is also important to note that collapse for attractive condensates can be arrested by controlling the number of atoms. Indeed, if the number of atoms in *each* potential trough is smaller than the critical number $\mathcal{N}_{cr}$ associated with the local potential, collapse is avoided [17,9].

The steady state for a single condensate inside a single-well potential V_j is a NLS soliton solution of the form [18]

$$u_{0;j}(x,t)=\sqrt{1-V_0}\,\mathrm{sech}(x-\xi_{0;j})e^{i(1/2-V_0)t}. \tag{3}$$

We consider the dynamics of a train of condensates $u(x,t)=\Sigma u_{0;j}(x,t)$ centered at the potential troughs $\xi_{0;j}$. For simplicity of presentation, we approximate the overall dynamics, focusing on two major contributions: (a) internal dynamics due to interactions between $u_{0;j}$ and V_j and (b) tail-tail interactions between consecutive solitons. We address each of these terms individually and use the linear superposition afforded by soliton perturbation theory [19]. Within our approximations (small tail-tail overlap) it is sensible to discard interactions between $u_{0;j}$ and V_k for $j\neq k$, and interactions between non-nearest neighbor condensates [19].

The evolution, for small perturbations, of the steady-state soliton $u_{0;j}$ inside its on-site potential V_j can be approximated by an oscillating soliton ansatz $u_j(x,t)=u_{0;j}(x-\xi_j,t)$ with constant height and width [20]. The position $\xi_j(t)$ for each condensate is then described by a particle inside an effective potential

$$\ddot{\xi}_j=-V'_{\rm eff}(\xi_j-\xi_{0;j}). \tag{4}$$

The effective potential $V_{\rm eff}$ may be obtained by soliton perturbation techniques, or alternatively, by demanding that the evolution of $\xi_j(t)$ in Eq. (3) respects the invariance of the NLS (2) energy

$$E=\int_{-\infty}^{+\infty}\left[\frac{1}{2}|u_x|^2-\frac{1}{2}|u|^4+|u|^2V(x)\right]dx. \tag{5}$$

It is well known [20] that the effective potential

$$V_{\rm eff}(\xi)\propto\int_{-\infty}^{+\infty}|u_{0,j}(x-\xi)|^2V_j(x)dx \tag{6}$$

is proportional to the overlapping integral between the displaced BEC density (3) and the on-site potential. Note that in Eq. (6), the on-site potential V_j is centered at $x=\xi_{0;j}$ and the BEC density $|u_{0;j}(x-\xi)|^2$ is centered at $x=\xi_{0;j}+\xi$ [see Eq. (3)]. The exact form of $V_{\rm eff}$ depends upon the on-site potential. For the particular case under consideration, $V_j(x)=V_0\tanh^2(x-\xi_{0;j})$, the effective potential admits the expansion $V_{\rm eff}(x)\propto\frac{4}{15}x^2-\frac{4}{63}x^4+o(x^6)$. More generally, the effective potential can be approximated, for small oscillations, by

$$V_{\rm eff}(x)=\frac{\alpha}{2}x^2+\frac{\beta}{4}x^4+o(x^6), \tag{7}$$

where α and β encode the shape information of V_j. In particular, even symmetry of $V_{\rm eff}$ is inherited from V_j.

Tail-tail interactions for neighboring condensates result in a complex version of the Toda lattice involving position and phases [21]. It is possible to further reduce the dynamics under the assumption that relative phases for consecutive condensates are constant. This is a reasonable approximation in the regime where the solitons are kept well apart [22]. In particular, we consider the case of a π phase shift between consecutive condensates, since in the steady state $(\xi_j=0)$ this configuration reduces to the Jacobi elliptic cosine that is known to be stable [18]. In contrast, a chain of condensates with zero phase shift reduces to the third Jacobi elliptic function, which is unstable [18]. With a relative phase of π, the tail-tail interactions reduce to a *real* Toda lattice [23] on the positions $\ddot{\xi}_j = 4(e^{-(\xi_j - \xi_{j-1})} - e^{-(\xi_{j+1}-\xi_j)})$. In practice, the π phase shift can be implemented by phase design on the initial configuration of the condensates [24]. From now on we consider that the amplitudes of oscillation of the condensates are small. Thus, since the steady state is stable, we eliminate the possibility of a condensate hopping to a neighboring lattice trough.

Exploiting the linearity of soliton perturbation theory we combine the on-site potential (4) with the tail-tail interactions to find a lattice differential equation on the condensate positions,

$$\ddot{\xi}_j = 4(e^{-(\xi_j - \xi_{j-1})} - e^{-(\xi_{j+1}-\xi_j)}) - V'_{\text{eff}}(\xi_j - \xi_{0,j}). \tag{8}$$

To find oscillatory solutions to Eq. (8), we use an oscillating ansatz [25], writing the position of the jth condensate as a combination of oscillatory modes $\xi_j(t) = \Sigma_k A_j(k)\cos(k\omega t)$ centered at $A_j(0) = \xi_{0,j}$. For small oscillations, a *one-mode* ansatz,

$$\xi_j(t) = \xi_{0,j} + A_j \cos(\omega t), \tag{9}$$

is sufficient to capture the essential dynamics. We substitute Eq. (9) into Eq. (8), expand and match terms to find a recurrence relation between the oscillation amplitudes A_j,

$$A_{j+1} = (a + bA_j^2)A_j - A_{j-1}, \tag{10}$$

with $a = 2 - \omega^2 + \alpha e^R/4$ and $b = 3\beta e^R/16$. We introduce $y_n = A_n$ and $x_n = A_{n-1}$, and recast the second-order recurrence relation (10) as the two-dimensional (2D) map M:

$$M: \begin{cases} x_{n+1} = y_n, \\ y_{n+1} = (a + by_n^2)y_n - x_n. \end{cases} \tag{11}$$

Up to the approximations made to obtain Eq. (10), solutions of Eq. (11) prescribe the amplitudes representing oscillatory solutions for the condensates. We remark that the oscillation frequency ω and the form of the on-site potential are incorporated through the parameters a and b of Eq. (10). In particular, one expects families of oscillatory solutions parametrized by their frequency ω.

We are interested in constructing *localized breathers* (localized oscillations) for the condensate dynamics. These solutions correspond to orbits homoclinic to the origin for the recurrence map (11). The corresponding orbits satisfy $A_0 \neq 0$ and $\lim_{n\to\pm\infty} A_n = 0$ with an exponential decay rate. A necessary condition for the existence of a homoclinic orbit is hyperbolicity of the origin. This is satisfied for all $|a| > 2$ or equivalently $|2 - \omega^2 + \alpha e^R/4| > 2$. This condition provides constraints on the intersite spacing R and breather frequency

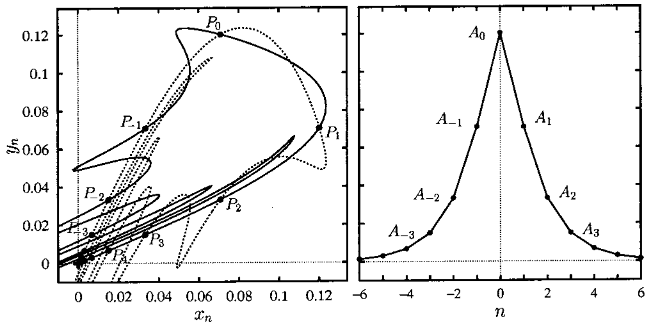

FIG. 2. Left: homoclinic tangle for the two-dimensional map (11). The homoclinic orbit $\{\ldots, P_{-1}, P_0, P_1, \ldots\}$ belongs to the stable (solid line) and unstable (dash line) manifolds. Right: the corresponding configuration for the oscillation amplitudes. ($R = 10$, $\omega = 17.671$, and $V_0 = 0.1$.)

ω for a given on-site trap V_j, which determines α. We find numerically, for reasonable values of R($R \approx$ a few condensate widths), that the stable (W^s) and unstable manifolds (W^u) of the origin intersect in a homoclinic tangle (see left panel in Fig. 2). Consider the trajectory of the two-dimensional map M that starts at the intersection point $P_0 \in W^s \cap W^u$ (see left panel in Fig. 2). From the invariance of the stable and unstable manifolds, each forward and backward iteration of P_0, labeled $\{\ldots, P_{-2}, P_{-1}, P_0, P_1, P_2, \ldots\}$ in Fig. 2, lies in the intersection. From area orientation it follows that this trajectory takes each second intersection [26]. The amplitudes for the localized oscillations are then given by the ordinates ($y_n = A_n$) of the homoclinic orbit (see right panel in Fig. 2).

The homoclinic orbit of the 2D map induces a breather on the condensate positions through the ansatz (9). An example of such localized oscillations for the condensates is depicted in Fig. 3, in which a central condensate oscillates with a maximal amplitude A_0 and the condensates on either side oscillate with amplitudes $A_{\pm n}$ that decrease exponentially with increasing n (see right panel in Fig. 2). The asymptotic decay rate for the oscillations ($\lambda_-^{|n|} = \lambda_+^{-|n|}$) is prescribed by

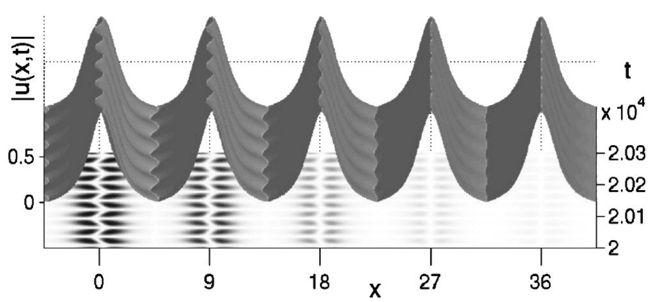

FIG. 3. Localized breathing oscillation in a chain of weakly coupled condensates in a periodic potential. This localized oscillation is obtained by full numerical solution of the Gross-Pitaevskii equation with an initial condition prescribed by our dynamical reduction. Only condensates with index 0 through 4 are shown (the oscillations are symmetric with respect to the condensate with index 0). The bottom plane depicts u_t—darker areas corresponds to regions where $u(x,t)$ undergoes greater temporal variation. ($R = 9$, $\omega \approx 0.11388$, and $V_0 = 0.025$.)

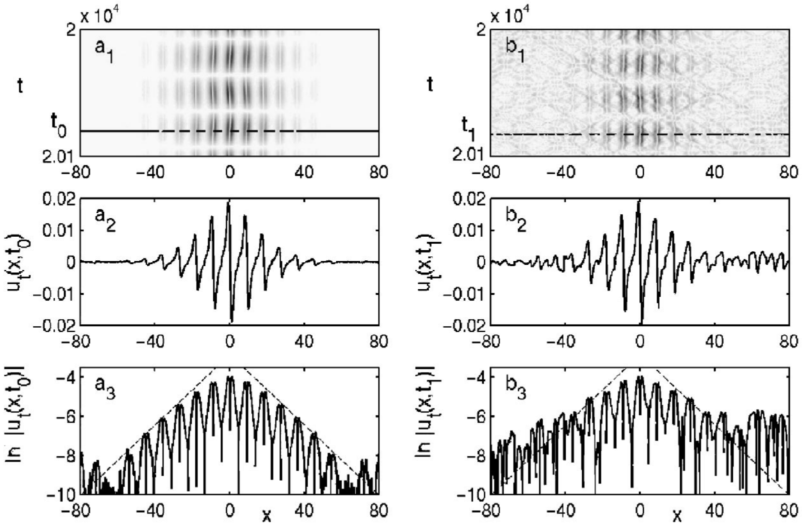

FIG. 4. Robustness of the perturbed localized breather in the Gross-Pitaevskii equation; (a) unperturbed and (b) perturbed. a_1 and b_1 depict a density plot of $|u_t(x,t)|$—darker areas correspond to larger $u(x,t)$ variations. Insets a_2 and a_3 depict $u_t(x,t_0)$ and $\ln(|u_t(x,t_0)|)$ at $t=t_0$ for the unperturbed system, whereas insets b_2 and b_3 depict the corresponding quantities at t_1 for the perturbed systems. Same parameter values as in Fig. 3.

the eigenvalues at the origin $\lambda_\pm=(a\pm\sqrt{a^2-4})/2$. Note that, because Eq. (11) has $x\leftrightarrow y$ symmetry, the breather is symmetric with respect to the central condensate $(\lambda_-=\lambda_+^{-1})$. We stress that the solution depicted in Fig. 3 is obtained by numerical integration of the full Gross-Pitaevskii equation (1) from initial conditions prescribed by the homoclinic orbit of our reduced 2D map. Due to the approximations used in our approach, orbits of the reduced 2D map are not *exact* solutions of the full GPE equation (1). Nevertheless, if we restrict our attention to small oscillations for weakly coupled BECs, there is a good correspondence between the reduced dynamics and the original Gross-Pitaevskii equation. This correspondence is reinforced by the structural stability of the orbits for the reduced 2D map (see below).

Localized breathers represent an important structure in the dynamics of the GPE equation describing a mechanism whereby energy and information can be pinned down on the periodic potential lattice. The occurrence of localized breathers in weakly coupled oscillatory units is a common phenomenon. Indeed, the existence of localized breathers has been formally established in general nonlinear Hamiltonian lattices of weakly interacting oscillators [27] by continuation from the so-called anticontinuum limit corresponding to the uncoupled case $(R=+\infty)$ [28]. The structural stability of the homoclinic tangle, arising from the transverse nature of the intersections of the stable and unstable manifolds, implies the persistence of the breather solution of the 2D map (11) under parameter changes, in particular, insuring the existence of the breather solution for the GPE. This persistence, together with the dynamic stability of the steady-state solution $(A_n=0)$, ensures the existence of the breather solution for the GPE. Therefore, despite the various approximations used in the reduction of the GPE to the 2D map (11), we observe localized breather oscillations in the original GPE dynamics (Fig. 3) for the predicted parameter values. More surprising is the robustness of the breathing dynamics to significant perturbations under the GPE dynamics (Fig. 4).

To demonstrate this robustness we construct the initial configuration (IC) as a concatenation of solitons with velocities, heights, widths, and positions predicted by our analysis, and with a π phase shift between consecutive solitons (as in Fig. 3). We perturb each soliton in the chain by adding a random value to each of the initial velocities, heights, widths, positions, and phases. The bounds for the perturbations correspond to (a) 15% of the *maximal* velocity on velocities, (b) 10% on heights, (c) 10% on widths, (d) 15% of the *maximal* amplitude $(0.15A_0)$ on positions, and (e) 15% of π on phases. Note that the perturbations on positions and velocities are proportional to the collective maximum and not to the individual values. After adding the perturbations, we concatenate the solitons and integrate the NLS (2) using a pseudospectral method. Additionally, we include (f) 5% (stationary) perturbation to the potential and (g) a noise level of 10^{-5} to $u(x,t)$ at *every* time step of the integration.

The total run is about 2×10^6 iterations. Figure 4 depicts the evolution of $u_t(x,t)$ for the unperturbed (left) and the perturbed (right) breather from direct simulations of the GPE equation. Despite the large perturbation to the IC and the additive noise, after a brief transient, the breather settles down and retains its localization with an approximate exponential decay (inset b_3). It is interesting to note that stronger perturbations to u did not necessarily destroy the localization, but often resulted in a slow excursion of the localized region along the lattice. The possibility of breather mobility in nonlinear lattices triggered by perturbations has been investigated previously [29].

The robustness of the localized breather dynamics presented above opens the possibility for experimental corroboration. The large perturbations to the IC result in an initial transient involving radiative losses, which would correspond experimentally to a small number of atoms being spilled away from the central cloud and absorbed by the noncondensed atoms at the periphery. After the transient, the breather settles down and retains its localization with an approximate exponential decay (inset b_3). While the breathers we constructed are robust to a wide host of perturbations, breathers are nongeneric in the sense that arbitrary initial conditions do not necessarily produce a breather. Also, with large enough perturbations the breathing phenomena are entirely destroyed.

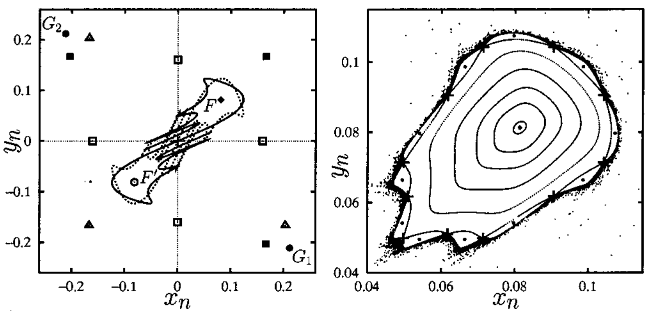

FIG. 5. Typical phase space for the reduced 2D map (11). Left: some periodic orbits and the homoclinic tangle. F and F' are fixed points, $\{G_1, G_2\}$ is a period-2 orbit. Some higher order periodic orbits are period 3 (triangles and filled squares) and period 4 (open squares). Right panel shows the behavior near the fixed point F (diamond). The map displays quasiperiodic orbits that disappear at the separatrix originating from the manifolds of a period-11 orbit (crosses). Outside this separation, a single chaotic orbit is depicted (small dots).

We may use the dynamical reduction described above to devise other breathing phenomena of Eq. (2). Within our approximations, any bounded nontrivial orbit of the 2D map M (11) gives rise to complex oscillatory behavior of the condensates in Eq. (2). In particular, periodic points of M correspond to *global* oscillations. The map M has three fixed points: the origin, $F=(x^*,x^*)$ and $F'=(-x^*,-x^*)$, where $x^*=\sqrt{(2-a)/b}$ (see Fig. 5). The fixed point at the origin gives rise to the trivial stationary solution $A_n=0$. The fixed points F and F' yield solutions in which all condensates oscillate in phase with the same amplitude x^*. The corresponding global breather for the original system (2) is depicted in Fig. 6(a). Other interesting orbits arise from higher-order periodic points. For example, the period-2 orbit $G_2=-M(G_1)=M^2(G_2)$ (see Fig. 5), where $G_1=(\hat{x},-\hat{x})$ and $G_2=(-\hat{x},\hat{x})$ with $\hat{x}=\sqrt{-(2+a)/b}$. This period-2 orbit corresponds to an amplitude configuration $\{\dots,\hat{x},-\hat{x},\hat{x},-\hat{x},\dots\}$, i.e., antiphase oscillations [see Fig. 6(b)]. It is in principle possible to construct more complex patterns for the global oscillations from higher-order periodic orbits of the 2D map (cf. Fig. 5).

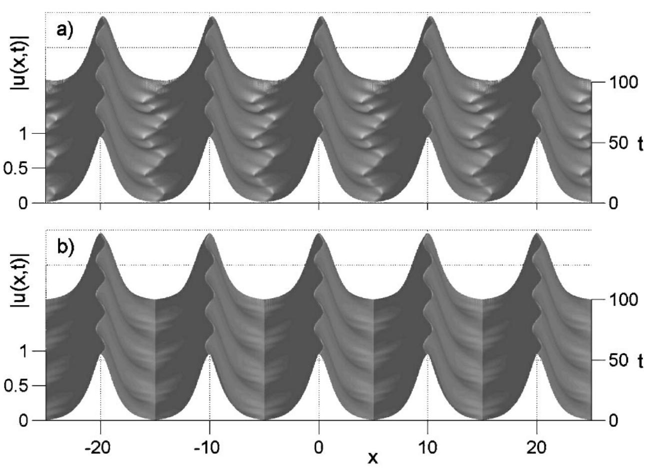

FIG. 6. Global oscillations of the condensates from simulations of the GPE equation. These global oscillations arise from periodic points of the reduced dynamics (11). (a) In-phase oscillations corresponding to the nontrivial fixed point F (see Fig. 5). (b) Antiphase oscillations corresponding to a period-2 cycle of Eq. (11) with alternating amplitude sign.

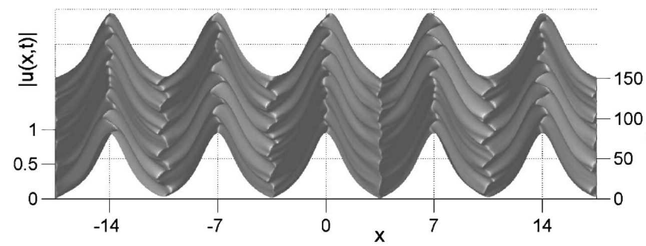

FIG. 7. Chaotic global oscillations of the condensates from GPE dynamics corresponding to the chaotic orbit of the reduced map (11) (see Fig. 5).

The 2D map also predicts global oscillations that are quasiperiodic in site index n. These orbits exist near the fixed point F (see Fig. 5, right panel). The corresponding breather for the full periodic NLS (2) has an in-phase global oscillation with a small modulation of the amplitudes (given by the rotation number of the quasiperiodic orbit around F). An interesting possibility for the dynamics of coupled condensates is the prospect of chaotic evolution. In a neighborhood of the fixed point F, there is a region containing chaotic orbits corresponding to chaotic oscillations for the condensates (see right panel in Fig. 5). This corresponds to chaotic oscillations for the condensates [see Fig. 7(c)]. It should be possible, in principle, to find the onset of chaos for the condensates by analyzing in more detail the reduced dynamics in Eq. (11).

We have constructed a variety of global and localized oscillatory behaviors of BECs in periodic potentials, identifying these solutions with orbits of a reduced 2D map. A key ingredient of the construction of localized oscillations is the existence of a homoclinic tangle. We demonstrate the surprising robustness of these solutions to perturbations. Since BEC experiments are quite delicate, we do not expect that direct manipulation could produce an exact initial condition corresponding to a localized oscillation. Nonetheless, we believe that localized oscillations may be observed in weakly coupled condensates that are appropriately engineered and then permitted to radiate away spurious energy. The techniques presented here can, in principle, be extended to lattices in higher dimensions such as vortex lattices. This has possible implications to modeling the interactions of atoms in optical traps that could potentially be used for quantum computing [30].

We are grateful to J. N. Kutz, B. Deconinck, P. G. Kevrekidis, P. Engels, and W. P. Reinhardt for providing stimulating discussions and relevant references. The authors acknowledge support from the Pacific Institute for the Mathematical Sciences and the NSERC Grant No. 611255 during the completion of this work.

[1] B. P. Anderson and M. A. Kasevich, Science **282**, 1686 (1998); D. Jaksch *et al.*, Phys. Rev. Lett. **81**, 3108 (1998).
[2] K. Berg-Sørensen and K. Mølmer, Phys. Rev. A **58**, 1480 (1998).
[3] A. Trombettoni and A. Smerzi, Phys. Rev. Lett. **86**, 2353 (2001).
[4] P. S. Jessen and I. H. Deutsch, Adv. At., Mol., Opt. Phys. **37**, 95 (1996); K. I. Petsas *et al.*, Phys. Rev. A **50**, 5173 (1994).
[5] J. Javanainen, Phys. Rev. A **60**, 4902 (1999).
[6] M. L. Chiofalo and M. P. Tosi, Phys. Lett. A **268**, 406 (2000).
[7] F. Kh. Abdullaev *et al.*, Phys. Rev. A **64**, 043606 (2001).
[8] E. P. Gross, Nuovo Cimento **20**, 454 (1961); L. P. Pitaevskii, Sov. Phys. JETP **13**, 451 (1961).
[9] F. Dalfovo *et al.*, Rev. Mod. Phys. **71**, 463 (1999).
[10] A. D. Jackson *et al.*, Phys. Rev. A **58**, 2417 (1998); V. Pérez-García *et al.*, *ibid.* **57**, 3837 (1998); M. Key *et al.*, Phys. Rev. Lett. **84**, 1371 (2000); N. H. Dekker *et al.*, *ibid.* **84**, 1124 (2000).
[11] P. A. Ruprecht *et al.*, Phys. Rev. A **51**, 4704 (1995).
[12] J. Reichel *et al.*, Phys. Rev. Lett. **83**, 3398 (1999); W. Hänsel *et al.*, *ibid.* **86**, 608 (2001); J. Reichel *et al.*, Appl. Phys. B: Lasers Opt. **B72**, 81 (2000).
[13] Th. Busch and J. R. Anglin, Phys. Rev. Lett. **84**, 2298 (2000); S. Burger *et al.*, *ibid.* **83**, 5198 (2000).
[14] B. Deconinck *et al.*, e-print cond-mat/0106231.
[15] M. Schiffer *et al.*, Appl. Phys. B: Lasers Opt. **B67**, 705 (1998); E. M. Wright *et al.*, Phys. Rev. A **63**, 013608 (2001).
[16] Collapse for attractive BECs is identified with the collapse of the NLS in dimensions $D \geqslant 2$. Since the NLS does not blow up in 1D, designing a trap that confines the BEC to an almost perfect 1D profile (a very thin cigar shape) could arrest, or at least delay, the collapse.
[17] C. C. Bradley *et al.*, Phys. Rev. Lett. **78**, 985 (1997).
[18] J. C. Bronski, L. D. Carr, R. Carretero-González, B. Deconinck, J. N. Kutz, and K. Promislow, Phys. Rev. E **64**, 056615 (2001).
[19] V. I. Karpman and V. Solov'ev, Physica D **3**, 142 (1981).
[20] R. Scharf and A. R. Bishop, Phys. Rev. E **47**, 1375 (1993); V. Pérez-García *et al.*, Phys. Rev. Lett. **77**, 5320 (1996).
[21] V. S. Gerdjikov *et al.*, Phys. Rev. E **55**, 6039 (1997); J. M. Arnold, *ibid.* **60**, 979 (1999).
[22] R. Carretero-González and K. Promislow, Discrete Contin. Dyn. Syst. Ser. B (to be published).
[23] M. Toda, *Theory of Nonlinear Lattices* (Springer, New York, 1989).
[24] J. Denschlag *et al.*, Science **287**, 97 (2000).
[25] Y. S. Kivshar, Phys. Rev. E **48**, R43 (1993); S. Flach and C. R. Willis, Phys. Rep. **295**, 181 (1998); T. Bountis *et al.*, Phys. Lett. A **268**, 50 (2000).
[26] The remaining intersections, the even ones, also give rise to a homoclinic orbit with a central portion consisting of two identical amplitudes [22].
[27] R. S. MacKay and S. Aubry, Nonlinearity **7**, 1623 (1994); S. Flach, Phys. Rev. E **51**, 1503 (1995).
[28] S. Aubry, Physica D **71**, 196 (1994).
[29] D. Chen *et al.*, Phys. Rev. Lett. **77**, 4776 (1996).
[30] I. H. Deutsch *et al.*, Fortschr. Phys. **48**, 923 (2000).